Trialkylsilylethynyl-Functionalized Tetraceno[2,3-*b*]thiophene and Anthra[2,3-*b*]thiophene Organic Transistors

Ming L. Tang,† Anna D. Reichardt,† Theo Siegrist,‡ Stefan C. B. Mannsfeld,§ and Zhenan Bao*,§

Departments of Chemistry and Chemical Engineering, Stanford University, 381 North-South Mall, Stanford, California 94305 and Bell Laboratories, Alcatel-Lucent, 600 Mountain Avenue, Murray Hill, New Jersey 07974

Received March 5, 2008. Revised Manuscript Received April 13, 2008

A series of ethynyl-substituted molecules with the tetraceno[2,3-*b*]thiophene and anthra[2,3-*b*]thiophene core have been synthesized. The aim was to investigate the impact of differently bulky side-chain substituents on the packing of the molecule in thin film and hence its thin-film transistor (TFT) mobility. Three R groups were used, namely, the tri-isopropyl-, triethyl-, and trimethylsilylethynyl groups. We did not observe a direct correlation between substituent size and TFT mobility. However, the 5,12-bis(tri-isopropylsilylethynyl)tetraceno[2,3-*b*]thiophene has a mobility as high as 1.25 $cm^2/V\cdot s$, the 5,12-bis(trimethylsilylethynyl)tetraceno[2,3-*b*]thiophene has a mobility of about 0.00616 $cm^2/V\cdot s$, while 5,10-bis(triethylsilylethynyl)anthra[2,3-*b*]thiophene and 5,10-bis(trimethylsilylethynyl)anthra[2,3-*b*]thiophene have a mobility of $10^{-4} cm^2/V\cdot s$ on phenylsilane- and octadecyltrichlorosilane-treated surfaces respectively.

Introduction

Organic semiconductors are promising as the next generation of electronic materials because they are amenable to large-area, low-cost processing.[1–4] This largely stems from the fact that the solubility of organic materials can be tuned by attaching various side chains to the conjugated core. Thus, one might imagine roll-to-roll processing of organic semiconductors for electronic applications that do not require the high mobility of crystalline silicon.[4]

Much thought has been put into designing molecules for organic light emitting diodes (OLEDs),[5] organic photovoltaics (OPVs),[6,7] and organic thin-film transistors (OTFTs).[1,3,4,8] Ideally, OTFTs would have mobilities on par with that of amorphous silicon (~1 $cm^2/V\cdot s$), high on/off ratios > 10^6, stability under ambient operating conditions, and solution processability. While several classes of molecules have shown promising performance, acene-based molecules have received the most attention because pentacene has shown the highest reported thin film mobility. Some of those that meet the above requirements[9] are 6,13-bis(tri-isopropylsilylethynyl)pentacene,[10] which has a mobility of 0.4 $cm^2/V\cdot s$ in an evaporated thin film, 2,6-bis[2-(4-pentylphenyl)vinyl]anthracene,[11] which has a mobility up to 1.28 $cm^2/V\cdot s$, functionalized anthradithiophene[12] molecules, which have solubilizing groups attached, and 6,13-bis(4-pentylphenylethynyl)pentacene,[13] which exhibits a mobility of 0.52 $cm^2/V\cdot s$ when drop cast from a chlorobenzene solution. All these molecules have high hole mobilities > 0.1 $cm^2/V\cdot s$, are soluble in common organic solvents, and appear to be stable under laboratory conditions.

We previously reported the synthesis of tetraceno[2,3-*b*]thiophene and anthra[2,3-*b*]thiophene.[14] They are designed to have pentacene-like structure except that the terminal fused benzene ring is replaced with a fused thiophene ring. These molecules have shown good thin-film field-effect mobility. In this work, we synthesized and studied the thin-film properties of six new bis(trialkylsilylethynyl)tetraceno[2,3-*b*]thiophene[15] and anthra[2,3-*b*]thiophene molecules. Previously, Anthony hypothesized that the ratio of the bulkiness of the substituents on the silylethynyl group, relative to the length of the conjugated core, affects the packing in thin film. It was observed that if the diameter of the spherical

---

* To whom correspondence should be addressed. E-mail: zbao@stanford.edu.
† Department of Chemistry, Stanford University.
‡ Bell Laboratories.
§ Department of Chemical Engineering, Stanford University.

(1) Dimitrakopoulos, C. D.; Malenfant, P. R. L. *Adv. Mater.* **2002**, *14*, 99+.
(2) Anthony, J. E. *Chem. Rev.* **2006**, *106*, 5028–5048.
(3) Murphy, A. R.; Frechet, J. M. J. *Chem. Rev.* **2007**, *107*, 1066–1096.
(4) Bao, Z.; Locklin, J. *Organic Field-Effect Transistors (Optical Science and Engineering Series)*, 1st ed.; CRC Press: Boca Raton, FL, 2007.
(5) Friend, R. H.; Gymer, R. W.; Holmes, A. B.; Burroughes, J. H.; Marks, R. N.; Taliani, C.; Bradley, D. D. C.; Dos Santos, D. A.; Bredas, J. L.; Logdlund, M.; Salaneck, W. R. *Nature* **1999**, *397*, 121–128.
(6) Hagfeldt, A.; Gratzel, M. *Acc. Chem. Res.* **2000**, *33*, 269–277.
(7) Hoppe, H.; Sariciftci, N. S. *J. Mater. Res.* **2004**, *19*, 1924–1945.
(8) Katz, H. E.; Bao, Z. N.; Gilat, S. L. *Acc. Chem. Res.* **2001**, *34*, 359–369.
(9) Afzali, A.; Dimitrakopoulos, C. D.; Breen, T. L. *J. Am. Chem. Soc.* **2002**, *124*, 8812–8813.
(10) Anthony, J. E.; Brooks, J. S.; Eaton, D. L.; Parkin, S. R. *J. Am. Chem. Soc.* **2001**, *123*, 9482–9483.
(11) Meng, H.; Sun, F. P.; Goldfinger, M. B.; Gao, F.; Londono, D. J.; Marshal, W. J.; Blackman, G. S.; Dobbs, K. D.; Keys, D. E. *J. Am. Chem. Soc.* **2006**, *128*, 9304–9305.
(12) Laquindanum, J. G.; Katz, H. E.; Lovinger, A. J. *J. Am. Chem. Soc.* **1998**, *120*, 664–672.
(13) Li, Y. N.; Wu, Y. L.; Liu, P.; Prostran, Z.; Gardner, S.; Ong, B. S. *Chem. Mater.* **2007**, *19*, 418–423.
(14) Tang, M. L.; Okamoto, T.; Bao, Z. N. *J. Am. Chem. Soc.* **2006**, *128*, 16002–16003.
(15) Palayangoda, S. S.; Mondal, R.; Shah, B. K.; Neckers, D. C. *J. Org. Chem.* **2007**, *72*, 6584–6587.

10.1021/cm800644y CCC: $40.75

substituent on the alkyne is one-half the length of the acene, then a 2-D "bricklayer" structure results, while if the size of the substituent is too big or too small, a 1-D "slipped-stacked" arrangement occurs. For example, for pentacene derivative **1**[10] the tri-isopropylsilyl (TIPS) substituent turns out to be very suitable, giving functionalized pentacene with thin film mobilities as high as 0.4 cm^2/V·s when vacuum deposited and 1.8 cm^2/V·s when drop cast from solution.[16] However, when the substituent is small, e.g., triethylsilyl (TES), or much bulkier, e.g., tri-*n*-propylsilyl, then a 1-D π-stack packing results;[17] if the size is increased even more to tri(trimethylsilyl)silyl, then a herringbone structure is observed. These molecules have a thin-film mobility of less than 0.001 cm^2/V·s. Similarly, the TESethynyl-substituted anthradithiophene **2**[18] grows in a 2-D π-stack structure and gives a drop-cast mobility of 1.0 cm^2/V·s, while other substituents on the alkyne do not give the desired packing and mobility.

It is of interest to investigate if the tetraceno[2,3-*b*]thiophene series follows similar trends. Here, we show that only TIPS on the alkyne results in a 2-D π-stack in the single crystal form, and TIPSethynyl tetraceno[2,3-*b*]thiophene (**TIPSEthiotet**) yields good transistors (mobilities as high as 1.25 cm^2/V·s when deposited as a thin film under high vacuum). Notably, though both the TES and trimethylsilyl (TMS) ethynyl tetraceno[2,3-*b*]thiophene (**TESEthiotet** and **TMSEthiotet**) form 1-D slip stacks in single crystals, thin films of **TESEthiotet** comprised of isolated grains and did not exhibit a measurable field effect, while **TMSEthiotet** gave a mobility of 0.00616 cm^2/V·s. This is not unexpected since in addition to the stacking motif the thin-film morphology is an important parameter influencing the performance of TFTs. Nucleation and growth of grains in the thin-film phase depend significantly on the kinetic processes occurring on the substrate surface. For the anthra[2,3-*b*]thiophene series, the TES and TMS ethynyl subsituents give an average of 10^{-4} cm^2/V·s on various silane-treated surfaces. This compares favorably to tetracene derivatives bearing two trimethoxyphenylethynyl substituents for which a hole mobility of 10^{-6} cm^2/V·s was measured in TFTs produced by spin coating.[19]

Experimental Details

Instrumentation. Nuclear magnetic resonance (NMR) spectra were recorded on an Varian Inova-500 MHz spectrometer. Chemical shifts (δ) are reported in parts per million, and the residual solvent peak was used as an internal standard. The Philips PANalytical X'Pert diffractometer with a PreFIX X-ray mirror at the incident beam and a parallel plate collimator at the diffracted beam was used on the thin films of the evaporated molecules. $\omega/2\theta$ scans were performed with Cu Kα radiation at a power of 45 mV and 40 mA with a step size of 0.02° and a step time of 1.0s. A Digital Instruments MMAFM-2 scanning probe microscope was used to perform tapping-mode AFM on the samples with a silicon tip of 300 kHz frequency. Cyclic voltammetry scans were recorded on a CHI411 instrument. UV−vis was recorded with a Varian Cary 6000i UV−vis spectrophotometer. Samples were prepared in ambient conditions with nonair-free cuvettes.

Crystallographic Investigations. Single crystals of the materials were analyzed using an Oxford-Diffraction Xcalibur 2 CCD diffractometer with graphite-monochromatized Mo Kα radiation. An Oxford-Diffraction Cryojet provided temperature control with data collection carried out in the range of 120−150 K.

FET Device Fabrication. Top contact devices were made according to a literature procedure.[20] A thermally grown dry silicon dioxide layer (300 nm) with a capacitance per unit area of 1.0×10^{-8} F/cm^2 functioned as the dielectric, while a heavily n-doped silicon substrate functioned as the gate electrode. Shadow masks with $W/L = 20$ ($W = 1000$ μm, $L = 50$ μm) were used after evaporation of the organic semiconductor to deposit the gold drain and source electrodes. The organic semiconductors were deposited at a rate of 0.2−0.3 Å/s under a pressure of $4-6 \times 10^{-6}$ Torr to a final thickness of 45 nm as determined in situ by a quartz crystal monitor. TFT measurements were performed in air using a Keithley 4200 semiconductor parameter analyzer.

Synthesis. All chemical reagents were purchased from Aldrich Chemical Co., TCI, Lancaster, or Alfa Aesar and used as received. Trialkylsilylacetylenes were purchased from GFS and used as received. All molecules were recrystallized three times in degassed hexanes prior to device fabrication.

5,12-Bis(tri-isopropylsilylethynyl)tetraceno[2,3-*b*]thiophene (**TIPSEthiotet**) was made according to literature methods.[10] Dark blue-purple powder; yield 69%. ^{1}H NMR (CDCl$_3$, 500 MHz): δ_H 9.32 (s, 2 H), 9.17 (s, 1 H), 9.13 (s, 1 H), 8.00 (m, 2 H), 7.54 (d, $J =$ 6.0 Hz, 1 H), 7.44 (m, 2 H), 7.41 (d, $J =$ 5.5 Hz, 1 H), 1.35 (s, 36H), 1.34 (s, 6 H) ppm. ^{13}C NMR (CDCl$_3$, 500 MHz): δ_C 140.42, 139.89, 132.32, 132.23, 130.61, 130.51, 130.50, 130.31, 130.29, 130.27, 128.95, 128.80, 126.43, 126.17, 126.12, 123.99, 121.59, 120.27, 118.84, 117.48, 106.82, 106.50, 104.61, 104.52, 19.19, 11.84 ppm. MS (+ESI/ APCI) *m/z*: 645.34 (MH$^+$). Anal. Calcd for $C_{42}H_{52}SSi_2$: C, 78.20; H, 8.12; S, 4.97. Found: C, 77.93; H, 8.13; S, 4.89.

5,10-Bis(tri-isopropylsilylethynyl)anthra[2,3-*b*]thiophene (**TIPSEthioant**) was prepared in the same manner as **TIPSEthiotet** above. Orange solid; yield 66%. ^{1}H NMR (CDCl$_3$, 500 MHz): δ_H 9.19 (s, 1 H), 9.15 (s, 1 H), 8.64 (m, 2 H), 7.57 (m, 2 H), 7.56 (d, $J =$ 6.0 Hz, 1 H), 7.44 (d, $J =$ 5.5 Hz, 1 H), 1.30 (s, 36 H), 1.29 (s, 6 H) ppm. ^{13}C NMR (CDCl$_3$, 500 MHz): δ_C 140.24, 139.90, 132.52, 132.31, 130.25, 130.15, 129.97, 127.53, 127.48, 126.84, 126.72, 123.94, 121.59, 120.32, 119.03, 117.82, 105.64, 105.39, 103.98, 103.90, 19.13, 11.77 ppm. MS (+ESI/ APCI) *m/z*: 595.33 (MH$^+$). Anal. Calcd for $C_{38}H_{50}SSi_2$: C, 76.70; H, 8.47; S, 5.39. Found: C, 75.09; H, 7.92; S, 5.26.

5,12-Bis(triethylsilylethynyl)tetraceno[2,3-*b*]thiophene (**TESEthiotet**) was prepared as follows. To dry hexanes (18.7 mL) under Ar(g) was added triethylsilylacetylene (0.263 g, 1.87 mmol). *n*-BuLi was added dropwise (1.05 mL, 1.68 mmol), and the reaction mixture was stirred for 1 h, after which dry hexanes (74 mL) and tetraceno[2,3-*b*]thiophene-5,12-dione (0.1 g, 0.318 mmol) were added in that order. The mixture was refluxed overnight. $SnCl_2 \cdot 2H_2O$ (0.464 g, 2.06 mmol) dissolved in 10% HCl(aq) was added, and the reaction mixture was refluxed for 1 h. The mixture was then quenched with water, extracted with dichloromethane, washed with brine, and dried with $MgSO_4$, and the solvent was removed under reduced pressure. The crude product was then run

---

(16) Park, S. K.; Kuo, C.-C.; Anthony, J. E.; Jackson, T. N. *2005 Int. Electron. Dev. Mtg. Technol. Digest* **2006**, 113.

(17) Anthony, J. E.; Eaton, D. L.; Parkin, S. R. *Org. Lett.* **2002**, *4*, 15–18.

(18) Payne, M. M.; Parkin, S. R.; Anthony, J. E.; Kuo, C. C.; Jackson, T. N. *J. Am. Chem. Soc.* **2005**, *127*, 4986–4987.

(19) Schmidt, R.; Gottling, S.; Leusser, D.; Stalke, D.; Krause, A. M.; Wurthner, F. *J. Mater. Chem.* **2006**, *16*, 3708–3714.

(20) Locklin, J.; Roberts, M. E.; Mannsfeld, S. C. B.; Bao, Z. *J. Macromol. Sci., Part C: Polym. Rev.* **2006**, *46*, 79–101.

Scheme 1. Synthesis of the Six Target Compounds, and Chemical Structures of Other Trialkylsilylethynyl Pentacene and Anthradithiophene Derivatives

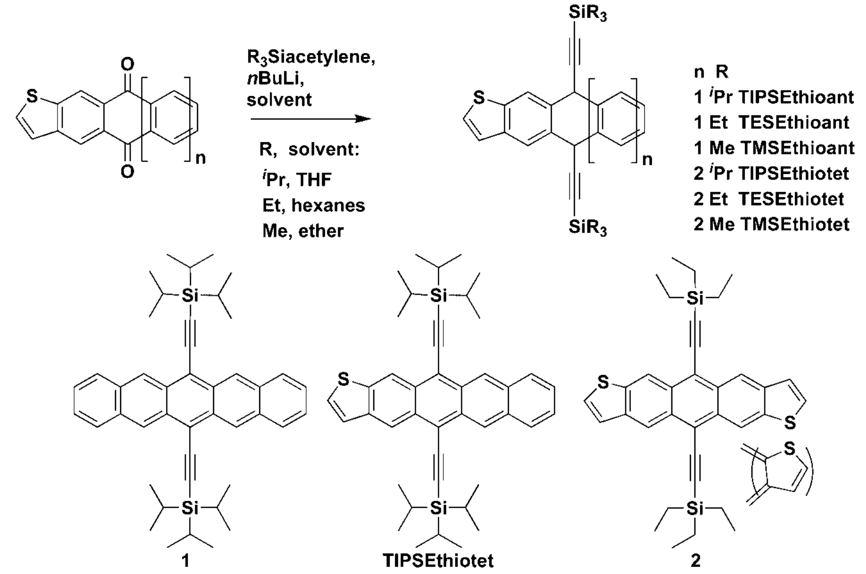

through a 1:4 dichloromethane:hexane silica gel column. A purple powder was collected (0.11 g, yield 60%). ^{1}H NMR (CDCl$_3$, 500 MHz): δ_H 9.28 (s, 2 H), 9.15 (s, 1 H), 9.10 (s, 1 H), 8.02 (m, 2 H), 7.54 (d, $J = 6.0$ Hz, 1 H), 7.44 (m, 2 H), 7.43 (d, $J = 5.5$ Hz, 1 H), 1.27 (td, $J = 8$ Hz, JJ=2 Hz, 18H), 0.94 (q, $J = 8.0$ Hz, 12 H) ppm. ^{13}C NMR (CDCl$_3$, 500 MHz): ^{13}C NMR (CDCl$_3$, 500 MHz): δ_C 140.46, 139.92, 132.33, 132.24, 130.63, 130.57, 130.53, 130.30, 130.25, 130.20, 128.82, 128.73, 126.36, 126.16, 126.04, 123.97, 121.53, 120.26, 118.72, 117.37, 107.83, 107.51, 104.07, 103.83, 8.08, 4.96 ppm. MS (+ESI/ APCI) *m/z*: 561.25 (MH$^+$). Anal. Calcd for $C_{36}H_{40}SSi_2$: C, 77.08; H, 7.19; S, 5.72. Found: C, 76.84; H, 7.32; S, 5.56.

5,10-Bis(triethylsilylethynyl)anthra[2,3-*b*]thiophene (**TESEthioant**) was prepared in the same manner as **TESEthiotet** above. Yellow-orange powder, 0.61 g; yield 58%. ^{1}H NMR (CDCl$_3$, 500 MHz): δ_H 9.16 (s, 1 H), 9.11 (s, 1 H), 8.61 (m, 2 H), 7.57 (m, 2 H), 7.57 (d, $J = 6.0$ Hz, 1 H), 7.47 (d, $J = 5.5$ Hz, 1 H), 1.22 (td, $J = 8$ Hz, $JJ = 2.5$ Hz, 18 H), 0.88 (q, $J = 8$ Hz, 12H) ppm. ^{13}C NMR (CDCl$_3$, 500 MHz): δ_C 140.25, 139.90, 132.43, 132.22, 130.23, 130.08, 129.99, 127.49, 127.44, 126.85, 126.73, 123.93, 121.50, 120.28, 118.88, 117.69, 106.64, 106.39, 103.24, 103.16, 8.01, 4.89 ppm. MS (+ESI/ APCI) *m/z*: 511.23 (MH$^+$). Anal. Calcd for $C_{32}H_{38}SSi_2$: C, 75.23; H, 7.50; S, 6.28. Found: C, 74.93; H, 7.51; S, 5.95.

5,12-Bis(trimethylsilylethynyl)tetraceno[2,3-*b*]thiophene (**TMSEthiotet**) was prepared as follows. To dry ether (11.5 mL) was added trimethylsilylacetylene (1.09 g, 11.13 mmol). *n*-BuLi was added dropwise (6.26 mL, 10.02 mmol), and the reaction mixture was stirred for 1 h, after which tetraceno[2,3-*b*]thiophene-5,12-dione (0.59 g, 1.89 mmol) was added. The mixture was refluxed overnight. $SnCl_2 \cdot 2H_2O$ (2.76 g, 12.23 mmol) dissolved in 10% HCl(aq) was added, and the reaction mixture was refluxed for 1 h. The mixture was then quenched with water, extracted with dichloromethane, washed with brine, and dried with $MgSO_4$, and the solvent was removed under reduced pressure. This crude product was then run through a 1:10 dichloromethane:hexane silica gel column. A purple powder was collected (0.60 g, yield 67%). ^{1}H NMR (CDCl$_3$, 500 MHz): δ_H 9.21 (s, 2 H), 9.11 (s, 1 H), 9.05 (s, 1 H), 8.06 (m, 2 H), 7.50 (d, $J = 5.5$ Hz, 1 H), 7.46 (m, 2 H), 7.44 (d, $J = 5.5$ Hz, 1 H), 0.52 (s, 18H), ppm. ^{13}C NMR (CDCl$_3$, 500 MHz): ^{13}C NMR (CDCl$_3$, 500 MHz): δ_C 140.48, 139.93, 132.31, 132.23, 130.39, 130.35, 130.30, 130.25, 130.22, 130.08, 128.84, 126.25, 126.22, 126.16, 126.12, 123.95, 121.43, 120.22, 118.52, 117.20, 110.13, 109.78, 102.81, 102.71, 0.53 ppm. MS (+ESI/ APCI) *m/z*: 477.15 (MH$^+$). Anal. Calcd for $C_{30}H_{28}SSi_2$: C, 75.57; H, 5.92; S, 6.73. Found: C, 75.28; H, 5.70; S, 6.74.

5,10-Bis(trimethylsilylethynyl)anthra[2,3-*b*]thiophene (**TMSEthioant**) was prepared in the same manner as **TMSEthiotet** above. Bright yellow-orange powder, 0.66 g; yield 74%.^{1}H NMR (CDCl$_3$, 500 MHz): δ_H 9.12 (s, 1 H), 9.06 (s, 1 H), 8.58 (m, 2 H), 7.58 (m, 2 H), 7.57 (d, $J = 6.0$ Hz, 1 H), 7.50 (d, $J = 5.5$ Hz, 1 H), 0.47 (s, 18H) ppm. ^{13}C NMR (CDCl$_3$, 500 MHz): δ_C 140.26, 139.90, 132.36, 132.16, 130.49, 130.05, 129.91, 129.80, 127.44, 126.88, 126.76, 123.93, 121.39, 120.23, 118.68, 117.51, 108.93, 108.65, 102.11, 102.02, 0.47 ppm. MS (+ESI/APCI) *m/z*: 427.14 (MH$^+$). Anal. Calcd for $C_{30}H_{28}SSi_2$: C, 75.57; H, 5.92; S, 6.73. Found: C, 75.43; H, 5.80; S, 6.43.

Results and Discussion

The TIPS-substituted molecules were synthesized according to literature methods[10] as shown in Scheme 1. However, for the TES and TMS groups, we found that tetrahydrofuran (THF) was not a good solvent as the reactions proceeded in low yield. For the TESacetylene, we used hexanes, while for the TMSacetylene, we found that ether was a good solvent to generate the acetylide. Yields of 60−70% were obtained. This may be because a more polar solvent is required to stabilize the TMSacetylide anion. These molecules were purified by three consecutive recrystallizations in degassed hexanes. Purification by sublimation resulted mainly in decomposition and a very low yield of the target compound.

The highest occupied molecular orbital (HOMO) levels were measured by cyclic voltammetry in a degassed solution of 0.1 M tetrabutylammonium hexafluorophosphate in *o*-dichlorobenzene at 100 °C. As expected, the HOMO levels were the same for **TIPSEthiotet**, **TESEthiotet**, and **TMSEthiotet** between −5.18 and −5.21 eV, while the HOMO levels for **TIPSEthioant**, **TESEthioant**, and **TMSEthioant** were beetween −5.41 and −5.44 eV. These levels were

Table 1. HOMO Levels, HOMO−LUMO Gaps in THF*, and Optical Bandgap, E_g* from an Evaporated 45 nm Thin Film on Quartz[a]

molecule	HOMO/ eV	HOMO−LUMO gap/ eV	E_g/ eV
TIPSEthiotet	−5.21	2.03	1.94
TESEthiotet	−5.20		1.96
TMSEthiotet	−5.18		1.90
TIPSEthioant	−5.41	2.42	2.33
TESEthioant	−5.42		2.34
TMSEthioant	−5.44		2.04

[a] The asterisk (*) denotes values taken from the absorption edge.

Table 2. Average Mobilities of at Least 10 Top-Contact Devices for TIPSEthiotet **and** TMSEthiotet **on Bare SiO_2 and OTS-Treated SiO_2 ($L = 50\mu$m, W/L = 20)**

molecule		SiO_2	OTS	T (°C)
TIPSE thiotet	μ (cm^2/V·s)	0.028 ± 0.003	0.11 ± 0.01	RT
	on/off	2E+04	9E+07	
	V_T/V	−1	−2	
	μ (cm^2/V·s)	0.801 ± 0.25	0.783 ± 0.17	60
	on/off	1E+05	7E+08	
	V_T/V	0−5	−(0−5)	
	μ (cm^2/V·s)	0.0514 ± 0.05	0.000461 ± 4E-4	90
	on/off	4E+03	1E+05	
	V_T/V	+20	−15	
TMSE thiotet	μ (cm^2/V·s)	7.3E-5 ± 1E-5	0.000545 ± 5E-5	RT
	in/off	9E+02	1E+04	
	V_T/V	−5	−20	
	μ (cm^2/V·s)	0.000301 ± 0.0001	0.00616 ± 0.001	60
	in/off	6E+04	2E+04	
	V_T/V	+(0−10)	−(10−20)	

measured against a ferrocene standard,[21] which was assumed to have a HOMO of −4.8 eV with respect to the vacuum level. UV−vis measurements in THF gave the same HOMO−LUMO gap of 2.03 eV for **TIPSEthiotet** and **TESEthiotet** and about 2.42 eV for **TIPSEthioant**, **TESEthioant**, and **TMSEthioant**, These results are summarized in Tables 1 and 2, which also list the optical band gaps for 45 nm vacuum-evaporated thin films. The thin-film optical bandgaps do not show a trend with substitution but instead center around 1.93 eV for the ethynyltetraceno[2,3-*b*]-thiophene and 2.33 eV for the ethynylanthra[2,3-*b*]-thiophene, indicating a slight red shift of less than 0.1 eV from solution to thin film.

Atomic force microscope (AFM) images of the vacuum-evaporated thin films are shown in Figures 1–8. As can be seen in Figure 3, for **TIPSEthiotet**, rough films formed at room temperature on both OTS-treated SiO_2 and bare SiO_2 with peak-to-peak height differences in excess of 100 nm. These films gave an average mobility of 0.11 and 0.028 cm^2/V·s for OTS and bare SiO_2, respectively. However, at a substrate temperature of 60 °C, on both surfaces, the films are smoother and exhibit more 2-D type of growth with the AFM-measured height corresponding to the measured QCM thickness. These continuous films give the best mobility, an average of 0.80 and 0.78 cm^2/V·s on bare SiO_2 and OTS-treated SiO_2. Interestingly, the highest mobility of 1.25 cm^2/V·s is measured on the SiO_2 surface not the OTS-treated surface. In comparison, **1**, 6,13-bis(tri-isopropyl)silylethynylpentacene exhibited the highest TFT mobility of 0.4 cm^2/V·s at 90 °C on OTS-treated SiO_2.[22] TFTs of both **1** and **TIPSEthiotet** exhibit significant contact resistance[22] even in the top-contact geometry, as shown from the nonlinear scaling of the square root of the source-drain current, $||I_{DS}||^{1/2}$, with gate voltage, V_G, in Figure 9. For compounds **1** and **TIPSEthiotet**, single-crystal structural analysis was performed. The packing motif in the crystals of these two compounds was a 2-D π-stacked structure with very similar $\pi-\pi$ stacking distances of 3.47 and 3.42 Å, respectively (see Figure 10). For the respective thin films, we observe distinct peaks in the out-of-plane (OOP) X-ray diffraction (XRD) spectra. Consistent with the general expectation that more crystalline films yield better device performance, we found that the smaller values of full-width-at-half-maximum (fwhm) and the higher peak intensities, the higher the mobility (Supporting Information). The interlayer *d* spacing is 16.4 Å for **TIPSEthiotet** and 16. 83 Å for compound **1**.[10]

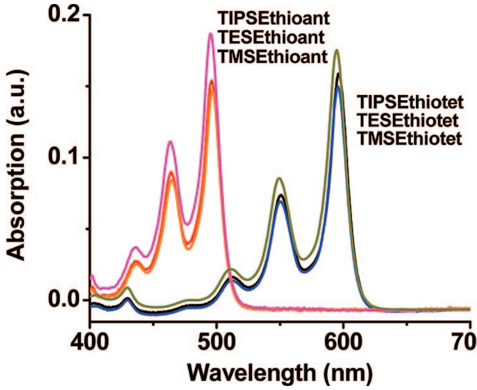

Figure 1. UV−vis spectra of the six target molecules in tetrahydrofuran at room temperature.

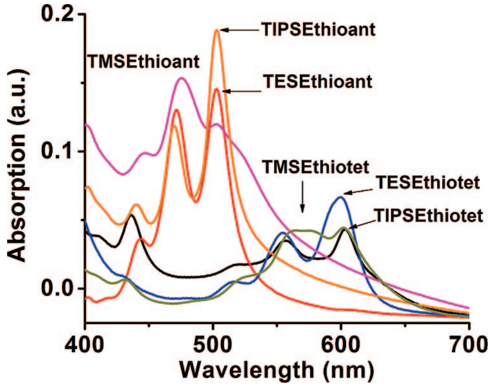

Figure 2. UV−vis spectra of 45 nm evaporated thin films of the six target molecules on quartz.

Unfortunately, no working **TESEthiotet** TFT device could be fabricated, and the lack of diffraction peaks in XRD spectra suggests that the **TESEthiotet** films were amorphous. We made thin films both at room temperature and at a 60 °C substrate temperature. Though the grains in films deposited at room temperature on SiO_2 appear connected by AFM (see Figure 4), we did not observe any field effect. At 60 °C (Figure 4), we observed isolated 3-D islands as high as 200 nm on OTS-treated SiO_2 and unconnected islands of about

---

(21) Thelakkat, M.; Schmidt, H. W. *Adv. Mater.* **1998**, *10*, 219+.

(22) Sheraw, C. D.; Jackson, T. N.; Eaton, D. L.; Anthony, J. E. *Adv. Mater.* **2003**, *15*, 2009–2011.

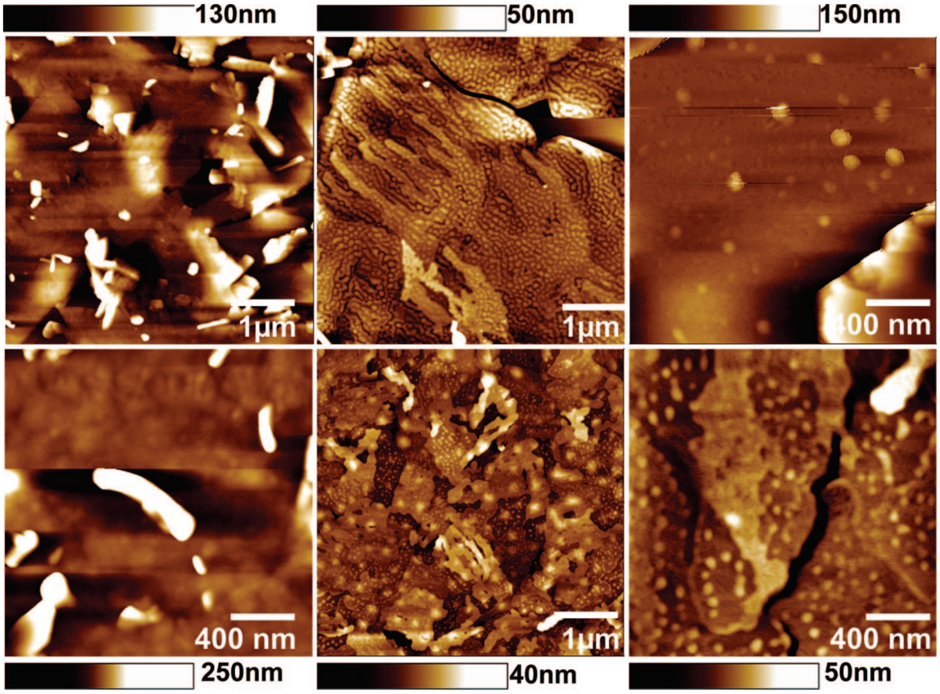

Figure 3. Thin films (45 nm) of **TIPSEthiotet** at a substrate temperature of RT (left), 60 °C (middle), and 90 °C (right): (top) OTS/ SiO_2, (bottom) SiO_2.

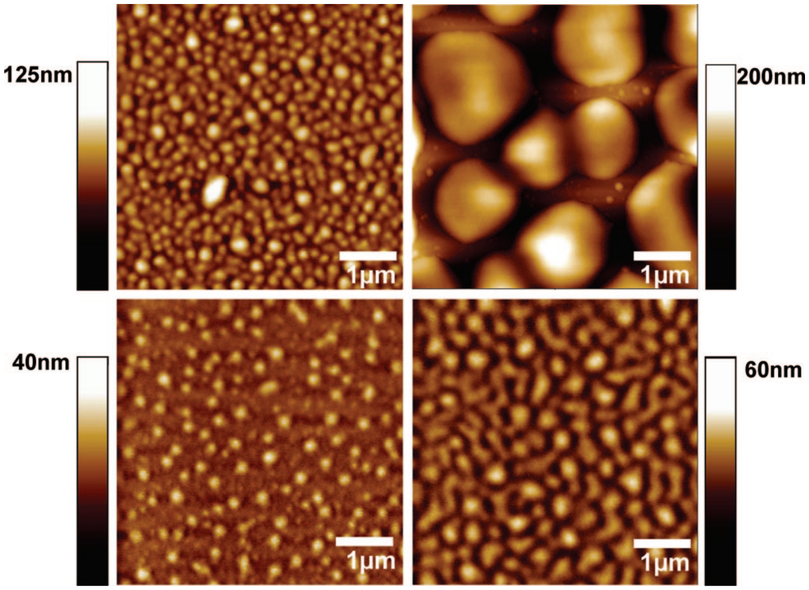

Figure 4. Thin films (45 nm) of **TESEthiotet** at a substrate temperature of RT (left) and 60 °C (right): (top) OTS/ SiO_2; (bottom) SiO_2.

50−60 nm height on bare SiO_2, which explains the lack of TFT performance.[23] Both **TESEthiotet** and **TMSEthiotet** display 1-D slip stacks in the single-crystal form. However, unlike **TESEthiotet**, evaporated thin films of **TMSEthiotet** show a pronounced XRD peak that corresponds to a *d* spacing of 13.4 Å, a smaller one at 10.6 Å, and an average field effect mobility of 0.00616 $cm^2/V \cdot s$. The AFM images in Figure 5 show that 2-D growth dominates at room temperature, and 3-D growth in the form of 250 nm grains tens of micrometers long is observed at a 60 °C substrate temperature. It appears that the grains are connected as mobility increases an order of magnitude from room temperature to an average of 0.00616 $cm^2/V \cdot s$ at a 60 °C substrate temperature.

For the ethynyl-anthra[2,3-*b*]thiophene series of molecules, 3-D island growth is very pronounced on OTS-treated SiO_2 surfaces, explaining the lack of any device mobility (Figures 6–8). For **TIPSEthioant**, we measure a rather small *d* spacing of 8.5 Å in the XRD spectra, which might be a sign of significantly tilted molecules, and again no working TFT could be fabricated (Figure 6). **TESEthioant** films are more crystalline films, and *d* spacings of 10.7 (001) and 5.4 Å (002) were measured, which are close to the *c* axis of the unit cell of 11.99 Å. AFM images of **TESEthioant** films are shown in Figure 7. Only on phenylsilane-treated SiO_2 did we obtain a field effect mobility of around 10^{-4} $cm^2/V \cdot s$. Similarly, for **TMSEthioant** only films deposited on OTS-treated SiO_2 substrates at room temperature showed

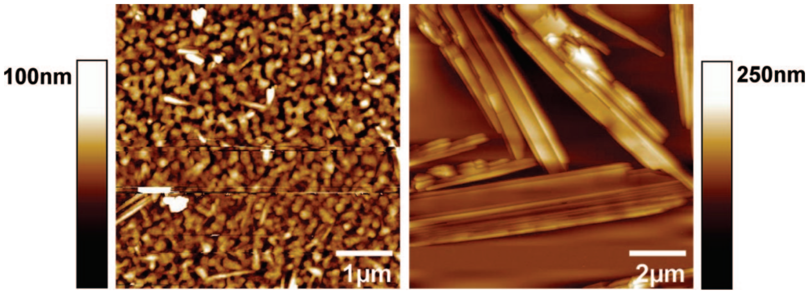

Figure 5. Thin films (33 nm) of **TMSEthiotet** on OTS/ SiO_2 at a substrate temperature of RT (left) and 60 °C (right).

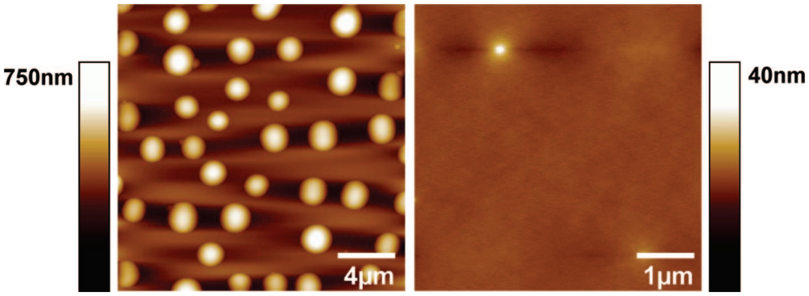

Figure 6. Thin films (45 nm) of **TIPSEthioant** at a substrate temperature of RT: (left) OTS/ SiO_2, (right) SiO_2.

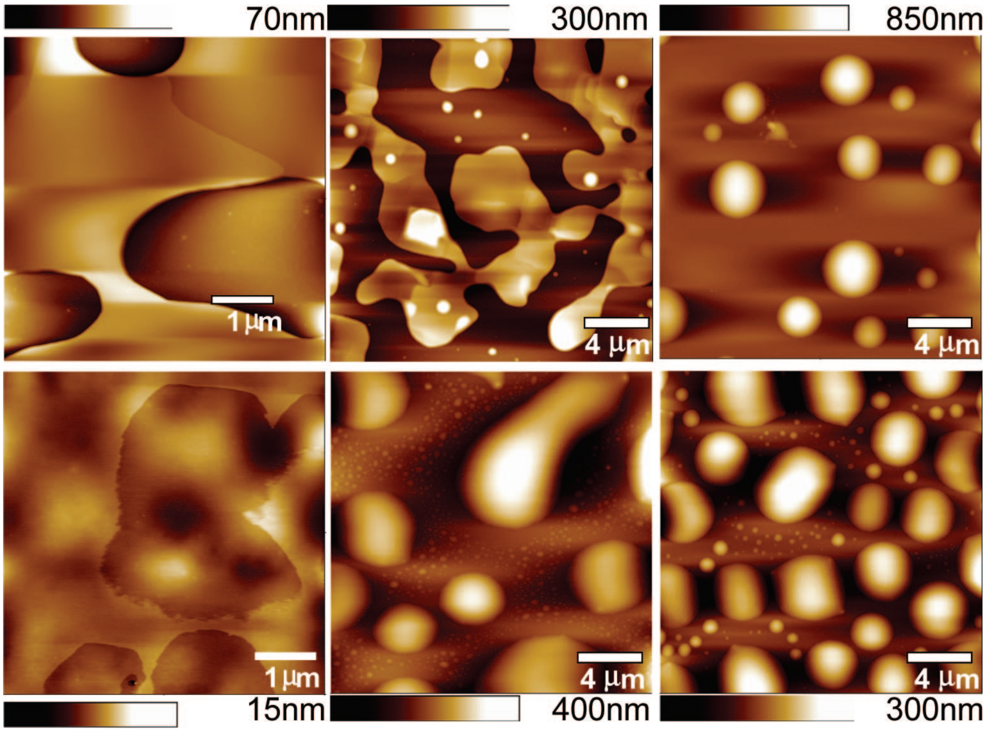

Figure 7. Thin films (45 nm) of **TESEthioant** at a substrate temperature of RT (left and middle) and 40 °C (right): (top left) aptes/SiO_2; (bottom left) phenylsilane/ SiO_2; (top middle and right) OTS/ SiO_2; (bottom middle and right) SiO_2.

10^{-4} $cm^2/V \cdot s$ mobility (AFM images in Figure 8). No pronounced peaks were observed in **TMSEthioant** thin-film XRD spectra, except a very small peak at 25.15°, which corresponds to a *d* spacing of 3.5 Å. These molecules exhibited on/off ratios on the order of 10^3 and higher threshold voltages than the tetraceno[2,3-*b*]thiophene series of molecules.

Discussion

Crystal structures have been obtained for all the molecules except **TMSEthioant**, which in our hands did not form crystals. Generally, the molecules in the structures show substantial disorder. Whereas the trialkylsilylethynyl part is well ordered, the aromatic backbone, due to its asymmetry, shows up to four different orientations. Rotation by 180° around the "5,12-axis" or the "5,10-axis" and rotation by 180° around the long axis of the aromatic system produces these four different orientations. Intuitively, the thiophene group can be found on either end of the aromatic backbone, both in the "up" and "down" sulfur orientation. The molecules are thus modeled using two "opposing" thiophene rings (joint occupation of 0.5) and a terminal phenyl ring

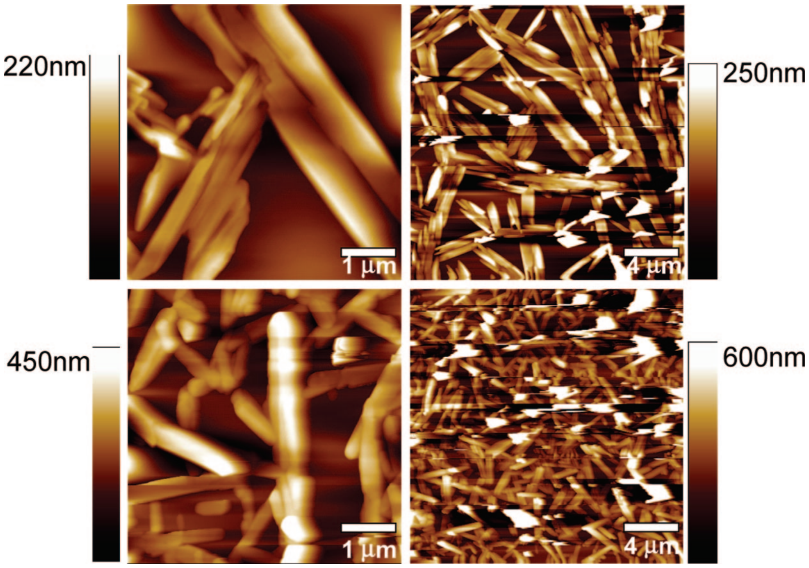

Figure 8. Thin films (45 nm) of **TMSEthioant** at a substrate temperature of RT: (top) OTS/ SiO$_2$, (bottom) SiO$_2$.

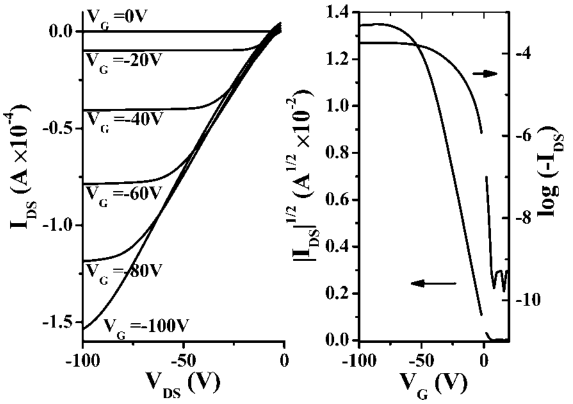

Figure 9. TFT curves of **TIPSEthiotet** on bare SiO$_2$ at a substrate temperature of 60 °C with $L = 50$ μm channel length and $W/L = 20$.

(occupation of 0.5). In this way, the observed electron density is adequately described for thiophene-tetracene systems. In contrast, the disorder is considerably larger for thiophene–anthracene systems, where the aromatic backbone is highly asymmetric, the thiophene end “sticking” out on either side, again in “up/down” sulfur orientation. Here, the trialkylsilylethynyl part is not as well defined as in the thiophene–tetracene systems; the molecules are displaced along the direction of the aromatic backbone depending on the orientation of the thiophene group. This is reflected in large atomic anisotropic displacement parameters with their largest displacement parallel to the long axis of the aromatic backbone. For this reason, the crystal structures of all the “**thioant**” systems only give an approximate location of the molecules in the crystal structure. However, the overall features are believed to be correct, and they are consistent with the “**thiotet**” systems.

Similar to **1**, 6,13-TIPSEpentacene, and **2**, TESEanthradithiophene, the **TIPSEthiotet** shows the “brick-work” structure that results in a two-dimensional arrangement of the molecules (see Figure 10). The **TIPS** group is large enough to prevent interdigitation, thus producing a “brick-type” slip-stack layer structure with the aromatic backbones separated by 3.40 Å. All molecules are oriented in the same way. In addition, one of the terminal methyl groups of the **TIPS** group is disordered. The XRD out-of-plane peak is 16.4–16.5 Å on device wafers, slightly smaller than the length of the *c* axis in the unit cell of 16.83 Å. Up to the (006) order was measured on devices made under different conditions, and no other peaks were observed. From this we conclude that the brick layers are oriented parallel to the substrate plane, an arrangement favorable to good charge transport between the source-drain contacts.

In contrast, **TESEthiotet** packs in individual slip stacks, where the aromatic backbone is separated from the adjacent molecule by 3.44 Å. As shown in Figure 10, the **TESE** groups are interdigitated, and the aromatic backbone makes an angle of 43.09° with the conjugated core in the nearest neighbor stacks. This kind of 1-D slip stack is not conducive to charge transport and may explain the lack of measurable field effect. Also in Figure 10, **TMSEthiotet** packs in 1-D slips stacks with a 3.38 Å distance between the aromatic backbones in a single stack and the TMSE groups interdigitating between the stacks. In contrast to **TESEthiotet**, the individual slip stacks are parallel to each other. This may explain why, when compared to **TIPSEthiotet**, which has a 2-D brick-layer structure, **TMSEthiotet** has an average of 2 orders of magnitude lower mobility, because its 1-D stack leads to 1-D grains in the thin film, increasing grain boundaries and thus lowering mobility.

For the **TMSEthiotet**, solution-grown crystals show two phases. The majority phase has a unit cell with the *c* axis 11.53 Å and *b* axis 9.99 Å, while the minority phase has unit cell with the *c* axis 16.83 Å and *b* axis 13.23 Å. On device wafers, from XRD, we found an intense peak that gave an out-of-plane *d* spacing of 13.4 Å (see Supporting Information). This corresponds to the minority phase. XRD also gives a much smaller peak with a *d* spacing of 10.6Å, which is compatible with the unit cell of the majority phase in solvent-grown crystals. We therefore conclude that **TMSEthiotet** is polymorphic, similar to pentacene.[24] The

---

(23) Horowitz, G.; Hajlaoui, M. E. *Adv. Mater.* **2000**, *12*, 1046–1050.

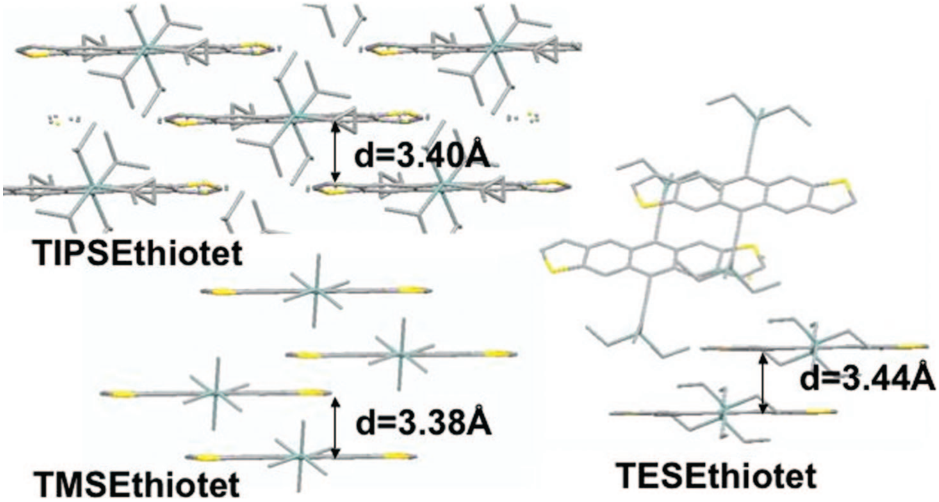

Figure 10. Single-crystal structures of **TIPSEthiotet**, which shows a 2-D bricklayer packing, **TESEthiotet**, which is a 1-D slip stack with neighboring stacks at an angle of 43.09° with each other and **TMSEthiotet**, a 1-D slip stack with neighboring stacks parallel to each other.

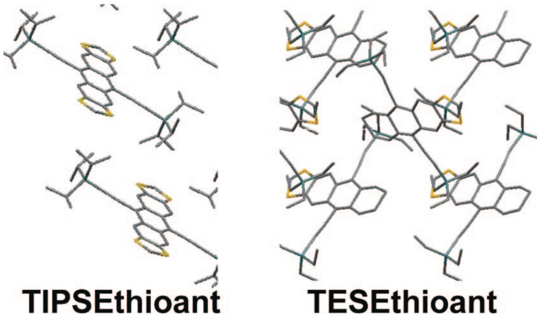

Figure 11. Single-crystal structures of **TIPSEthioant** and **TESEthioant**, which are disordered. The molecules pack in slip stacks.

polymorphism observed in thin films is also observed in solution-grown crystals. However, the two unit cells are closely related, and the polymorphism may be due to ordering of the thiophene ring due to the different preparation methods.

The structures of **TIPSEthioant** and **TESEthioant** cannot be refined to an acceptable level due to the substantial disorder in the aromatic backbone, as mentioned above. They are included for reference only since intermolecular distances and angles are not reasonable as they cannot be accurately determined. However, it is possible to extract distances between planes defined by the aromatic backbones since these planes are not influenced severely by the disorder. As shown in Figure 11, **TIPSEthioant** molecules pack in slip stacks with the distance between the aromatic backbone on the order of 3.40 Å and the TIPSE groups interdigitating between the stacks. No bricklayer-type packing is observed, in contrast to **TIPSEthiotet**. The molecular packing allows for the disorder, but the packing density is not optimal due to different orientations possible for the molecules. The **TESEthioant** structure again is strongly interdigitated, resulting in a large distance between aromatic backbones (5.63Å). Furthermore, these stacks have alternating tilts with the angle between the aromatic backbones on the order of 64.6°. Since the molecule is highly asymmetric, its location within the lattice is not well defined: a high degree of disorder is observed and may be correlated to the fact that no field effect was seen in the thin films.

Conclusions

We made a series of ethynyl-substituted molecules from the tetraceno[2,3-*b*]thiophene and anthra[2,3-*b*]thiophene core. The **TIPS**-substituted tetraceno[2,3-*b*]thiophene **TIPSEthiotet** has an average mobility of 0.80 $cm^2/V \cdot s$, a maximum mobility of 1.25 $cm^2/V \cdot s$, is stable,[15] is very soluble, and exhibits a 2-D bricklayer structure in single crystals. The **TMSEthiotet** molecule has a mobility of $10^{-3} cm^2/V \cdot s$, with a 1-D slip stack in single-crystal form. The other molecules exhibit negligible to low mobility on the order of 10^{-4} $cm^2/V \cdot s$, most likely due to strong disorder in molecular packing and dewetting film morphology on SiO_2 or chemically modified SiO_2 substrates leading to unconnected films. This study indicates that the thin-film morphology is extremely sensitive to the molecular structure. Further work is being done to elucidate the structure−property relationships that govern film morphology and polymorphism in evaporated thin films.

Acknowledgment. M.L.T. thanks Melbourne Lemieux for making the phenylsilane and aptes surfaces. She acknowledges a Kodak graduate fellowship. A.R. acknowledges a Major grant from Stanford University's Undergraduate Academic Life office. S.C.B. acknowledges financial support from the Deutsche Forschungsgemeinschaft. Z.B. acknowledges partial financial support from the Global Climate and Energy Project (GCEP), the Stanford Center for Polymer Interfaces and Macromolecular Assemblies (NSF-Center MRSEC under Award DMR- 0213618), and an AFSOR grant.

Supporting Information Available: All XRD scans, a table summarizing the 2*θ* peak positions and the corresponding *d* spacings, as well as device curves for **TMSEthiotet**, **TESEthioant**, and **TMSEthioant**. This material is available free of charge via the Internet at http://pubs.acs.org.

CM800644Y

---

(24) Siegrist, T.; Besnard, C.; Haas, S.; Schiltz, M.; Pattison, P.; Chernyshov, D.; Batlogg, B.; Kloc, C. *Adv. Mater.* **2007**, *19*, 2079+.